Ab initio potential energy surface for the carbon dioxide molecule pair and thermophysical properties of dilute carbon dioxide gas

Robert Hellmann

Institut für Chemie, Universität Rostock, 18059 Rostock, Germany

---

Abstract

A four-dimensional intermolecular potential energy surface (PES) for two rigid carbon dioxide molecules was determined from quantum-chemical *ab initio* calculations. Interaction energies for 1229 CO_2–CO_2 configurations were computed at the CCSD(T) level of theory using basis sets up to aug-cc-pVQZ supplemented with bond functions. An analytical site-site potential function with seven sites per CO_2 molecule was fitted to the interaction energies. The PES was validated by calculating the second virial coefficient as well as viscosity and thermal conductivity in the dilute-gas limit.

Keywords: carbon dioxide, potential energy surface, second virial coefficient, kinetic theory, viscosity, thermal conductivity

© 2014. This manuscript version is made available under the CC-BY-NC-ND 4.0 license
`http://creativecommons.org/licenses/by-nc-nd/4.0/`

The Version of Record is available at `http://dx.doi.org/10.1016/j.cplett.2014.08.057`.

---

1. Introduction

The thermophysical properties of a dilute gas are governed solely by binary interactions and therefore by the intermolecular pair potentials. Today, potential energy surfaces (PESs) for pairs of small molecules can be determined with very high accuracy using quantum-chemical *ab initio* methods. Once the pair potentials are available, it is possible to calculate, for example, second virial coefficients using statistical thermodynamics or transport and relaxation properties in the dilute-gas limit utilizing the kinetic theory of gases [1].

Several *ab initio* PESs for the carbon dioxide molecule pair have been developed in recent years [2–6]. The potentials of Bock et al. [3] and Oakley and Wheatley [4] were developed utilizing the supermolecular approach at the MP2 level of theory, whereas symmetry-adapted perturbation theory (SAPT) [7] was used by Bukowski et al. [2], Yu et al. [5], and Wang et al. [6]. Wang et al. also employed the highly accurate supermolecular CCSD(T)-F12 approach [8, 9]. The CO_2 molecules were treated as rigid rotors in all of these studies.

In the present Letter, a new four-dimensional rigid-rotor PES for the carbon dioxide molecule pair is presented. It is based on supermolecular calculations for a large number of CO_2–CO_2 configurations using the CCSD(T) method [9]. Basis sets up to quadruple-zeta quality with bond functions were applied, and the resulting interaction energies were extrapolated to the complete basis set (CBS) limit. A site-site potential function with seven sites per CO_2 molecule was fitted to the computed interaction energies. Both the site-site interaction parameters and the positions of the sites were fully optimized. The potential function was used to calculate the second virial coefficient and the shear viscosity and thermal conductivity in the dilute-gas limit. The results are compared with those for the potentials of Bock et al. and Bukowski et al. as well as with selected experimental data.

2. Intermolecular potential

2.1. Ab initio calculations

In all quantum-chemical *ab initio* calculations the zero-point vibrationally averaged geometry of CO_2, characterized by a C–O bond length of 1.1625 Å, was used. We determined this value as follows. First, a geometry optimization was performed at the all-electron CCSD(T) level with the cc-pwCVQZ basis set [10], resulting in an equilibrium bond length of 1.1602 Å. Then a cubic force field calculation at the same level of theory was performed, yielding a vibrationally averaged bond length of 1.1626 Å. The difference between these two values was then added to a highly accurate *ab initio* value of 1.1601 Å [11] for the equilibrium bond length.

Each configuration of two rigid CO_2 molecules can be expressed by the four variables R, θ_1, θ_2, and ϕ (illustrated in Figure 1), where R is the distance between the centers of mass of the two molecules, θ_1 and θ_2 are the angles between the R axis and the bond axes of molecules 1 and 2, respectively, and ϕ is the dihedral angle. The range of the angles can be restricted to $0^\circ \leqslant \theta_1 \leqslant \theta_2 \leqslant 90^\circ$ and $0^\circ \leqslant \phi \leqslant 180^\circ$ due to symmetry. A

Email address: `robert.hellmann@uni-rostock.de` (Robert Hellmann)

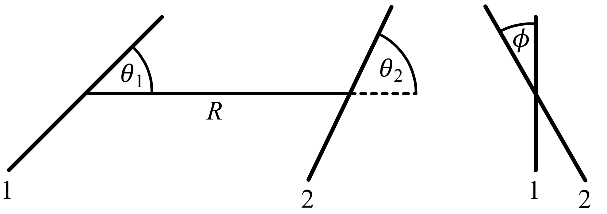

Figure 1: Internal coordinates of the CO_2 molecule pair.

total of 60 distinct angular configurations were considered. The angles θ_1 and θ_2 were varied in steps of 22.5°, and ϕ was varied in steps of 22.5° for $\theta_1 > 45°$, of 30° for $\theta_1 = 45°$, and of 45° for $\theta_1 < 45°$. The number of center-of-mass separations R considered for each angular configuration varies from 15 in the range $3.75\ \text{Å} \leqslant R \leqslant 12\ \text{Å}$ (for $\theta_1 = \theta_2 = 0°$) to 23 in the range $1.75\ \text{Å} \leqslant R \leqslant 12\ \text{Å}$ (e.g., for $\theta_1 = \theta_2 = \phi = 90°$). This resulted in a total of 1229 CO_2–CO_2 configurations.

The interaction energies $V(R, \theta_1, \theta_2, \phi)$ were computed utilizing the supermolecular approach including the full counterpoise correction [12] at the frozen-core CCSD(T) level of theory with the aug-cc-pVXZ basis sets with $X = 3$ and $X = 4$ [13, 14]. Both basis sets were supplemented by a 3s3p2d1f set of bond functions located midway along the R axis with exponents of 0.1, 0.3, and 0.9 for s and p, 0.25 and 0.75 for d, and 0.45 for f. The correlation contributions to the interaction energies, $V_{\mathrm{CCSD(T)\,corr}}$, were extrapolated to the CBS limit using the two-point extrapolation scheme of Halkier et al. [15],

$$V_{\mathrm{CCSD(T)\,corr}}(X) = V^{\mathrm{CBS}}_{\mathrm{CCSD(T)\,corr}} + \alpha X^{-3}. \tag{1}$$

The HF contributions were not extrapolated, since they converge much faster to the CBS limit than the correlation contributions. Therefore the HF interaction energies from the aug-cc-pVQZ calculations were used to approximate the CBS limit.

All *ab initio* calculations were performed using the CFOUR program [16]. The computed interaction energies for the 1229 configurations are given in the Supplementary information.

2.2. *Analytical potential function*

A site-site potential function with seven sites per CO_2 molecule was fitted to the calculated interaction energies. This corresponds to four different types of sites and ten different types of site-site combinations. The functional form for each site-site interaction is

$$\begin{aligned} V_{ij}(R_{ij}) =& A_{ij} \exp(-\alpha_{ij} R_{ij}) - f_6(b_{ij}, R_{ij}) \frac{C_{6\,ij}}{R_{ij}^6} \\ & - f_8(b_{ij}, R_{ij}) \frac{C_{8\,ij}}{R_{ij}^8} + \frac{q_i q_j}{R_{ij}}, \end{aligned} \tag{2}$$

where R_{ij} is the distance between site i of molecule 1 and site j of molecule 2. The damping functions f_n are given by [17]

$$f_n(b_{ij}, R_{ij}) = 1 - \exp(-b_{ij} R_{ij}) \sum_{k=0}^{n} \frac{(b_{ij} R_{ij})^k}{k!}. \tag{3}$$

Table 1: Equilibrium structure of the CO_2 dimer (with $\theta_1 = \theta_2 = \theta$ and $\phi = 0°$) for different potential functions.

Pair potential	R/Å	θ/deg	D_e/K
Bukowski et al. (SAPT-a) [2]	3.54	59.0	696.8
Bock et al. [3]	3.47	59.8	694.6
Oakley and Wheatley (CBS-a) [4]	3.51	58	679
Wang et al. [6]	3.50	56.9	785
This work, V_A	3.530	58.64	724.5
This work, V_B	3.533	58.60	723.5

The total interaction potential is the sum over all site-site interactions,

$$V(R, \theta_1, \theta_2, \phi) = \sum_{i=1}^{7} \sum_{j=1}^{7} V_{ij} \left[R_{ij}(R, \theta_1, \theta_2, \phi) \right]. \tag{4}$$

The parameters A, α, b, C_6, and C_8 for the ten different site-site combinations as well as the site charges q and the positions of the sites were fully optimized in a non-linear least-squares fit to the 1229 computed interaction energies. Three constraints were imposed:

1. The total charge of the monomers had to be zero.
2. The quadrupole moment of the monomers had to be equal to a value of -3.16323 a.u. resulting from an *ab initio* calculation at the frozen-core CCSD(T)/aug-cc-pV5Z level.
3. The isotropic average of the C_6 dispersion coefficient, $C_{6\,\mathrm{iso}} = \sum_{i=1}^{7} \sum_{j=1}^{7} C_{6\,ij}$, had to be equal to the accurate value of 158.7 a.u. [18] from dipole oscillator strength distributions (DOSDs).

The potential function thus obtained is denoted by V_A. Using highly accurate experimental data for the second virial coefficient as guidance (see Section 3), we obtained an improved potential function, V_B, by replacing the term αX^{-3} in Eq. 1 by $\alpha X^{-3.2}$ and refitting the potential parameters. Figure 2 illustrates the distance dependence of the CCSD(T) interaction energies in the CBS limit (obtained with the adjusted exponent) and the fitted potential function V_B. The interaction energies are given in Kelvin, i.e., they have been divided by Boltzmann's constant k_B. In Figure 3 interaction energies calculated using V_B are plotted against the corresponding CCSD(T)/CBS values for energies up to 20 000 K. The deviations from a straight line are very small, demonstrating the high quality of the fit.

The parameters of the equilibrium structure of the CO_2 dimer are listed in Table 1 for the potential functions V_A and V_B, as well as for the potentials of Bukowski et al. (SAPT-a fit) [2], Bock et al. [3], Oakley and Wheatley (CBS-a fit) [4], and Wang et al. [6]. The equilibrium dissociation energies D_e for V_A and V_B, which differ by only about 1 K, are significantly larger than those for the other potentials, with the exception of the potential of Wang et al., for which D_e is much higher.

The parameters of the potential functions V_A and V_B, the interaction energies calculated with these functions for all 1229 investigated configurations, as well as a Fortran 90 code for evaluating V_A and V_B are provided in the Supplementary information.

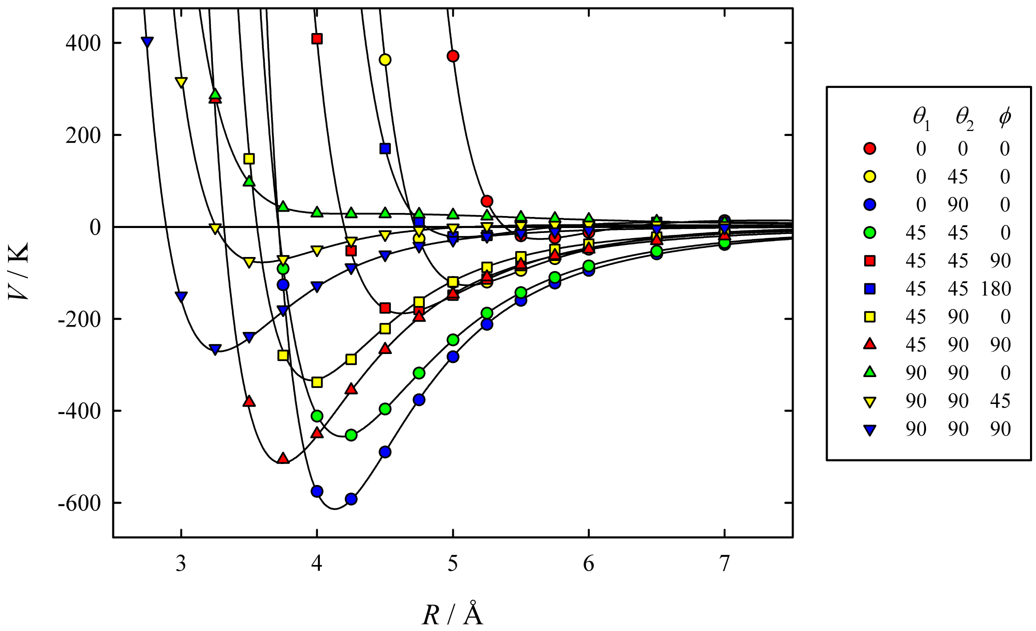

Figure 2: CO_2–CO_2 pair potential as a function of the distance R for various angular configurations. The CCSD(T) interaction energies in the CBS limit are represented by symbols and the fitted analytical potential function V_B by solid lines.

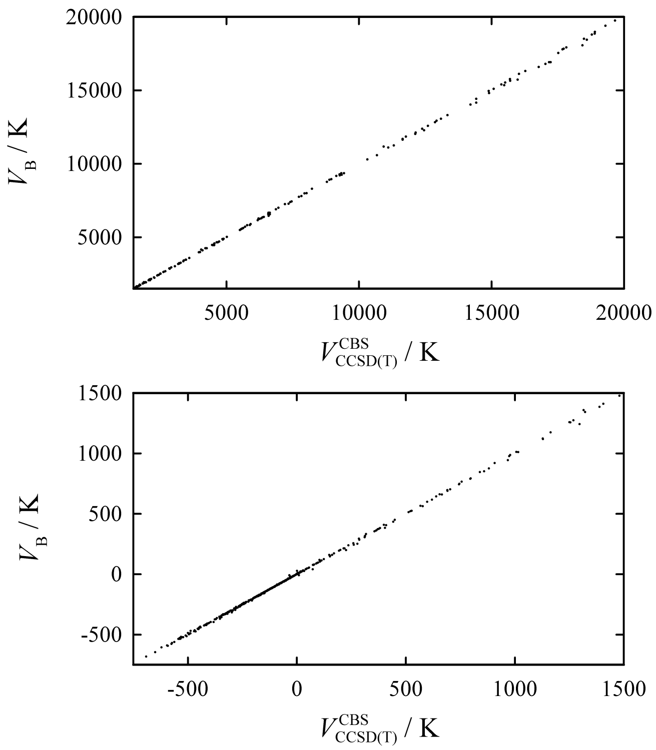

Figure 3: Interaction energies from the fitted analytical potential function V_B versus the corresponding CCSD(T)/CBS values.

3. Second virial coefficient

The classical second virial coefficient for a gas composed of rigid molecules is given by

$$B_{cl}(T) = -\frac{N_A}{2} \int_0^\infty \langle f_{12} \rangle_{\Omega_1,\Omega_2} d\mathbf{R}, \tag{5}$$

with

$$f_{12} = \exp\left[-\frac{V(\mathbf{R}, \Omega_1, \Omega_2)}{k_B T}\right] - 1, \tag{6}$$

where $\mathbf{R}$ is the distance vector between the centers of mass of the two molecules, Ω_1 and Ω_2 represent the angular orientations of molecules 1 and 2, respectively, and the angle brackets denote an average over Ω_1 and Ω_2. Quantum effects can be taken into account by replacing the pair potential V in Eq. 6 by the quadratic Feynman–Hibbs (QFH) effective pair potential [19]. For identical rigid linear molecules it can be written as

$$\begin{aligned} V_{QFH}(T) =& V + \frac{\hbar^2}{12 k_B T}\left[\frac{1}{m}\left(\frac{\partial^2 V}{\partial x^2} + \frac{\partial^2 V}{\partial y^2} + \frac{\partial^2 V}{\partial z^2}\right)\right. \\ &\left. + \frac{1}{2I} \sum_{i=1}^{2} \left(\frac{\partial^2 V}{\partial \psi_{i,a}^2} + \frac{\partial^2 V}{\partial \psi_{i,b}^2}\right)\right], \end{aligned} \tag{7}$$

where m and I are the molecular mass and moment of inertia, respectively, x, y, z are the Cartesian components of $\mathbf{R}$, and the angles $\psi_{i,a}$ and $\psi_{i,b}$ correspond to rotations around two arbitrarily chosen principal axes a and b of molecule i, with the restriction that a and b are perpendicular to each other.

The second virial coefficient of carbon dioxide was computed for 89 temperatures in the range from 150 K to 2000 K

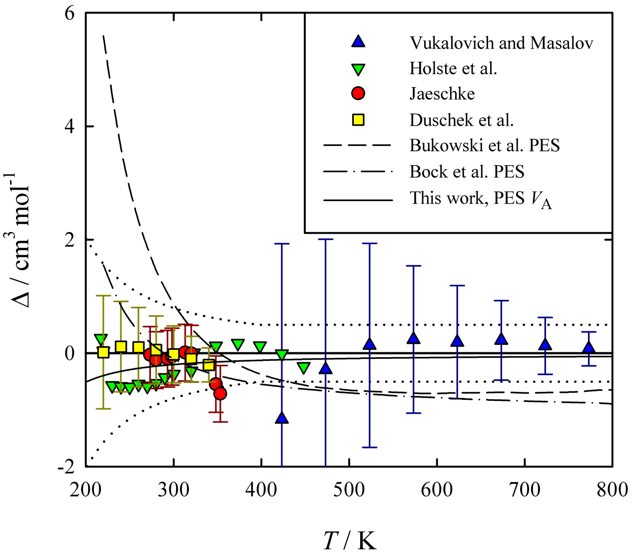

Figure 4: Deviations, $\Delta = B - B^{V_B}_{\mathrm{QFH}}$, of experimental data and calculated values for the second virial coefficient of CO_2 from values computed using the potential function V_B. The dotted lines indicate the estimated uncertainties of $B^{V_B}_{\mathrm{QFH}}$.

using the Mayer-sampling Monte Carlo (MSMC) approach of Singh and Kofke [20]. Results for all temperatures were obtained simultaneously by performing multi-temperature simulations [20–22] with a sampling temperature of 150 K and 5×10^{10} trial moves. In each MC trial move one of the molecules was displaced and rotated, and the maximum step size for the moves was adjusted in short equilibration periods to achieve acceptance rates of 50%. The second derivatives of the pair potential in Eq. 7 were evaluated analytically. As a reference system, the hard-sphere fluid with $\sigma = 4.5$ Å was chosen. Calculated virial coefficients from 16 independent simulation runs were averaged. The final results are converged within 0.02 cm^3 mol^{-1} for all temperatures. They are listed for both V_A and V_B in the Supplementary information.

In Figure 4 selected experimental data [23–26] for the second virial coefficient of carbon dioxide are compared with the computed values $B^{V_A}_{\mathrm{QFH}}$ and $B^{V_B}_{\mathrm{QFH}}$ (interpolated for the experimental temperatures). The values of Vukalovich and Masalov [23] were taken from Ref. [27]. Data close to room temperature of Jaeschke [25] and Duschek et al. [26] were used as reference for the fine tuning of the PES (see Section 2.2). The agreement between the experimental data and both $B^{V_A}_{\mathrm{QFH}}$ and $B^{V_B}_{\mathrm{QFH}}$ is excellent over most of the temperature range. Our estimate of the uncertainties of $B^{V_B}_{\mathrm{QFH}}$ is given by

$$\delta B^{V_B}_{\mathrm{QFH}} = \max\left(a_1 \left|B^{V_B}_{\mathrm{QFH}} - B^{V_A}_{\mathrm{QFH}}\right|, a_2, a_3 T\right), \tag{8}$$

where $a_1 = 4$, $a_2 = 0.5$ cm^3 mol^{-1}, and $a_3 = 5 \times 10^{-4}$ cm^3 mol^{-1} K^{-1}.

Figure 4 also shows deviations for second virial coefficients calculated by Bock [28] for the potentials of Bukowski et al. [2] and Bock et al. [3]. Bock used the approach of Pack [29] to account for quantum effects instead of the QFH approach employed in the present work. However, this should only have a very small effect on the resulting virial coefficients. The potential of Bukowski et al. yields second virial coefficients that are too positive at low temperatures and too negative at high temperatures. For the potential of Bock et al. the virial coefficients are mostly within experimental error bars, but at higher temperatures they are also too negative.

4. Shear viscosity and thermal conductivity

Transport properties in the dilute-gas limit can be calculated using the kinetic theory of molecular gases [1]. The shear viscosity η is given as

$$\eta(T) = \frac{k_B T}{\langle v \rangle_0} \frac{f_\eta^{(n)}}{\mathfrak{S}(2000)}, \tag{9}$$

where $\langle v \rangle_0 = 4(k_B T/\pi m)^{1/2}$ is the average relative thermal speed, and $\mathfrak{S}(2000)$ is a temperature-dependent generalized cross section. The quantity $f_\eta^{(n)}$ is an nth-order correction factor that accounts for higher basis function terms in the perturbation series expansion of the solution of the Boltzmann equation [1]. It is given by

$$f_\eta^{(n)} = \mathfrak{S}(2000) \frac{S_{11}^{(n)}}{S^{(n)}}, \tag{10}$$

where $S^{(n)}$ is a determinant of cross sections and $S_{11}^{(n)}$ its minor. In the second-order approximation, which results from including the basis functions $\mathbf{\Phi}^{2000}$, $\mathbf{\Phi}^{2010}$, $\mathbf{\Phi}^{2001}$, and $\mathbf{\Phi}^{0200}$, we have [30, 31]

$$S^{(2)} = \begin{vmatrix} \mathfrak{S}(2000) & \mathfrak{S}\binom{2000}{2010} & \mathfrak{S}\binom{2000}{2001} & \mathfrak{S}\binom{2000}{0200} \\ \mathfrak{S}\binom{2010}{2000} & \mathfrak{S}(2010) & \mathfrak{S}\binom{2010}{2001} & \mathfrak{S}\binom{2010}{0200} \\ \mathfrak{S}\binom{2001}{2000} & \mathfrak{S}\binom{2001}{2010} & \mathfrak{S}(2001) & \mathfrak{S}\binom{2001}{0200} \\ \mathfrak{S}\binom{0200}{2000} & \mathfrak{S}\binom{0200}{2010} & \mathfrak{S}\binom{0200}{2001} & \mathfrak{S}(0200) \end{vmatrix}. \tag{11}$$

In the present work, we employ a third-order approximation that includes the basis functions $\mathbf{\Phi}^{2000}$, $\mathbf{\Phi}^{2010}$, $\mathbf{\Phi}^{2001}$, $\mathbf{\Phi}^{0200}$, $\mathbf{\Phi}^{2020}$, $\mathbf{\Phi}^{2011}$, $\mathbf{\Phi}^{2002}$, $\mathbf{\Phi}_2^{2100}$, and $\mathbf{\Phi}_2^{2200}$. This results in a 9×9 determinant $S^{(3)}$ similar in structure to $S^{(2)}$. Note that the basis functions $\mathbf{\Phi}_2^{2100}$ and $\mathbf{\Phi}_2^{2200}$ were not considered in the third-order approximation given in Ref. [31].

The thermal conductivity λ was evaluated in a second-order approximation using a recently derived expression in terms of generalized cross sections [32] that takes the contributions of the vibrational degrees of freedom more accurately into account than the previous approach given in Refs. [33] and [34]. Both approaches require knowledge of the vibrational contribution to the isochoric heat capacity in the ideal-gas limit, $C^0_{\mathrm{vib}} = C^0_V - 5k_B/2$. Values of C^0_V for CO_2 were obtained from the equation of state of Span and Wagner [35].

The generalized cross sections needed to evaluate viscosity and thermal conductivity were computed by means of classical trajectories using a modified version of the TRAJECT software code [36]. For a given total energy, $E = E_{\mathrm{tr}} + E_{\mathrm{rot}}$, classical trajectories describing the collision process of two molecules were obtained by integrating Hamilton's equations for linear rigid rotors from pre- to post-collisional values (initial and final separation: 500 Å). The total-energy-dependent generalized cross sections can be represented as nine-dimensional integrals over the initial states. They were calculated for 33 values of E, ranging from 60 K to 60 000 K, by means of a simple Monte Carlo procedure, in which the initial states were generated utilizing quasi-random numbers. Up to 4×10^6 trajectories were computed at each energy. The number of trajectories had to be reduced significantly for low energies, because the computational demand to achieve a sufficient accuracy for a particular trajectory increases as the energy decreases. The final integration over E to obtain the temperature-dependent generalized cross sections was performed using Chebyshev quadrature. We estimate the precision of the resulting transport property values to be 0.1% for viscosity and 0.2% for thermal conductivity. Values obtained for both properties with the potential function V_{B} are given in the Supplementary information for 173 temperatures between 150 K and 2000 K. The corresponding values for V_{A} agree within ±0.02% for all temperatures with those for V_{B}.

In Figure 5 selected experimental data [37–39] and a correlation [40] for the shear viscosity of dilute CO_2 are compared with values obtained for the potential function V_{B}. Maitland and Smith [37] measured the viscosity of CO_2 relative to that of nitrogen at each temperature. We reanalyzed these measurements using viscosity values for nitrogen recommended in Ref. [22]. The viscosity values of Hendl et al. [39] were measured with an oscillating-disk viscometer, which was calibrated using an old reference value for the viscosity of CO_2 at room temperature. These measurements were reevaluated by Vogel [41] using a highly accurate *ab initio* value for the viscosity of helium at room temperature [42].

The comparison with the experimental data reveals that the calculated values are too small, but have the correct temperature dependence. The average deviation of the reevaluated data of Hendl et al. from the calculated values is +0.55%. Hence, for practical applications, we propose a simple scaling of the calculated values by a factor of 1.0055. We estimate the uncertainty of the scaled values to be 0.2% between 300 K and 700 K, increasing to about 1% at both 150 K and 2000 K.

Also shown in Figure 5 are the deviations for viscosity values computed by Bock et al. [40] for the potentials of Bukowski et al. [2] and of Bock et al. [3] using the TRAJECT code [36]. The values for the potential of Bukowski et al. show nearly the same temperature dependence as the values for the potential function V_{B} and agree even better with the experimental data, whereas the values for the potential of Bock et al. exhibit a different temperature dependence than the experimental data and the values obtained with the other two potential functions.

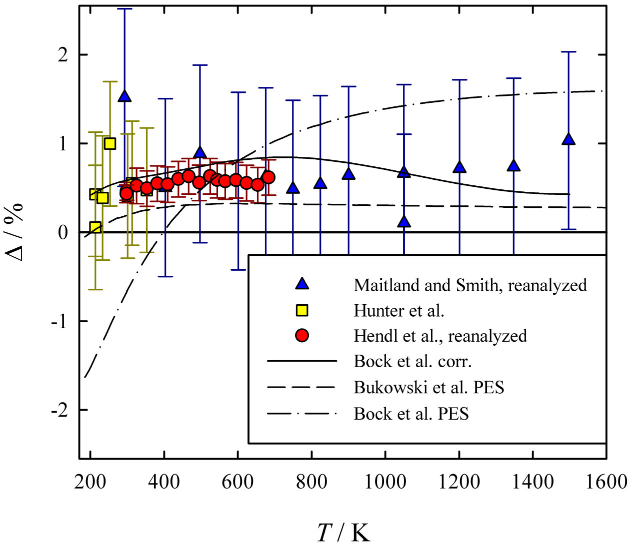

Figure 5: Relative deviations, $\Delta = (\eta - \eta^{V_{\mathrm{B}}})/\eta^{V_{\mathrm{B}}}$, of experimental data, a correlation, and calculated values for the shear viscosity of dilute CO_2 from values computed using the potential function V_{B}.

In Figure 6 selected experimental data [43–47] for the thermal conductivity of dilute CO_2, as well as a correlation [48] and values computed by Bock et al. [34] for the potentials of Bukowski et al. [2] and of Bock et al. [3] are compared with values obtained for the potential function V_{B}. The figure reveals that most of the experimental data sets are not mutually consistent within their stated uncertainties. We believe that the most reliable data are those reported by Haarman [44] and Li et al. [47], since their thermal conductivity data for argon and nitrogen, which are reported in the same papers, agree within ±0.5% with values obtained for highly accurate pair potentials [22, 49]. As in the case of the viscosity, we propose a scaling of the calculated values. A scaling factor of 1.011 seems to be optimal, as it results in thermal conductivity values that are consistent with the data of Haarman [44] and Li et al. [47], as well as with most of the data of Johnston and Grilly [43] and with the datum closest to room temperature of Millat et al. [46]. We estimate the uncertainty of the scaled values to be 1% between 300 K and 700 K, increasing to 2% at both 150 K and 2000 K. This uncertainty estimate does not take into account the increase of the thermal conductivity due to partial dissociation [50] of CO_2 at high temperatures.

The deviations of the thermal conductivity values computed by Bock et al. [34] for the potentials of Bukowski et al. [2] and of Bock et al. [3] are similar to those observed for viscosity. The values obtained for the potential of Bukowski et al. [2] are slightly closer to the experimental data than the values calculated for the potential function V_{B}.

5. Summary and conclusions

A new four-dimensional intermolecular potential for two rigid carbon dioxide molecules was determined utilizing quantum-chemical *ab initio* calculations. Interaction energies were computed for 1229 CO_2–CO_2 configurations at the

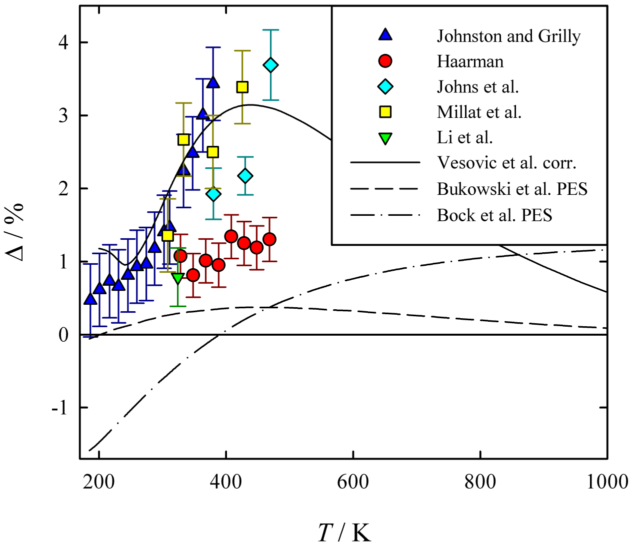

Figure 6: Relative deviations, $\Delta = (\lambda - \lambda^{V_{\rm B}})/\lambda^{V_{\rm B}}$, of experimental data, a correlation, and calculated values for the thermal conductivity of dilute CO_2 from values computed using the potential function $V_{\rm B}$.

CCSD(T) level of theory. Basis sets up to aug-cc-pVQZ, supplemented by bond functions between the two molecules, were employed and the resulting interaction energies were extrapolated to the complete basis set limit. A site-site potential function with seven sites per molecule and isotropic site-site interactions was fitted to the calculated interaction energies.

To validate the new potential function, the second virial coefficient as well as shear viscosity and thermal conductivity in the dilute-gas limit were computed for temperatures between 150 K and 2000 K. For the second virial coefficient, very good agreement was obtained with highly accurate experimental data. These data were also used for a fine tuning of the potential. In the case of the two transport properties, the comparison with the most accurate experimental data suggests that the computed values for viscosity and thermal conductivity are too low by about 0.5% and 1%, respectively. These deviations are probably caused primarily by the deficiencies of the rigid-rotor approximation. Since the relative deviations are only weakly temperature dependent, a simple scaling of the computed transport property values is proposed to obtain highly accurate values for practical applications.

Acknowledgment

This work was financially supported by the Deutsche Forschungsgemeinschaft, Grant No. HE 6155/1-1.

Appendix A. Supplementary data

Supplementary data associated with this article can be found, in the online version, at `http://dx.doi.org/10.1016/j.cplett.2014.08.057`.

References

[1] F. R. W. McCourt, J. J. M. Beenakker, W. E. Köhler, I. Kuščer, Nonequilibrium Phenomena in Polyatomic Gases, volume I: Dilute Gases, Clarendon Press, Oxford, 1990.
[2] R. Bukowski, J. Sadlej, B. Jeziorski, P. Jankowski, K. Szalewicz, S. A. Kucharski, H. L. Williams, B. M. Rice, J. Chem. Phys. 110 (1999) 3785–3803.
[3] S. Bock, E. Bich, E. Vogel, Chem. Phys. 257 (2000) 147–156.
[4] M. T. Oakley, R. J. Wheatley, J. Chem. Phys. 130 (2009) 034110.
[5] K. Yu, J. G. McDaniel, J. R. Schmidt, J. Phys. Chem. B 115 (2011) 10054–10063.
[6] F.-F. Wang, R. Kumar, K. D. Jordan, Theor. Chem. Acc. 131 (2012) 1132.
[7] B. Jeziorski, R. Moszynski, K. Szalewicz, Chem. Rev. 94 (1994) 1887–1930.
[8] T. B. Adler, G. Knizia, H.-J. Werner, J. Chem. Phys. 127 (2007) 221106.
[9] K. Raghavachari, G. W. Trucks, J. A. Pople, M. Head-Gordon, Chem. Phys. Lett. 157 (1989) 479–483.
[10] K. A. Peterson, T. H. Dunning, Jr., J. Chem. Phys. 117 (2002) 10548–10560.
[11] M. Heckert, M. Kállay, D. P. Tew, W. Klopper, J. Gauss, J. Chem. Phys. 125 (2006) 044108.
[12] S. F. Boys, F. Bernardi, Mol. Phys. 19 (1970) 553–566.
[13] T. H. Dunning, Jr., J. Chem. Phys. 90 (1989) 1007–1023.
[14] R. A. Kendall, T. H. Dunning, Jr., R. J. Harrison, J. Chem. Phys. 96 (1992) 6796–6806.
[15] A. Halkier, T. Helgaker, P. Jørgensen, W. Klopper, H. Koch, J. Olsen, A. K. Wilson, Chem. Phys. Lett. 286 (1998) 243–252.
[16] cfour, Coupled-Cluster techniques for Computational Chemistry, a quantum-chemical program package by J. F. Stanton, J. Gauss, M. E. Harding, P. G. Szalay with contributions from A. A. Auer, R. J. Bartlett, U. Benedikt, C. Berger, D. E. Bernholdt, Y. J. Bomble, L. Cheng, O. Christiansen, M. Heckert, O. Heun, C. Huber, T.-C. Jagau, D. Jonsson, J. Jusélius, K. Klein, W. J. Lauderdale, D. A. Matthews, T. Metzroth, L. A. Mück, D. P. O'Neill, D. R. Price, E. Prochnow, C. Puzzarini, K. Ruud, F. Schiffmann, W. Schwalbach, S. Stopkowicz, A. Tajti, J. Vázquez, F. Wang, J. D. Watts and the integral packages molecule (J. Almlöf and P. R. Taylor), props (P. R. Taylor), abacus (T. Helgaker, H. J. Aa. Jensen, P. Jørgensen, and J. Olsen), and ECP routines by A. V. Mitin and C. van Wüllen. For the current version, see http://www.cfour.de.
[17] K. T. Tang, J. P. Toennies, J. Chem. Phys. 80 (1984) 3726–3741.
[18] B. L. Jhanwar, W. J. Meath, Chem. Phys. 67 (1982) 185–199.
[19] R. P. Feynman, A. R. Hibbs, Quantum Mechanics and Path Integrals, McGraw-Hill, New York, 1965.
[20] J. K. Singh, D. A. Kofke, Phys. Rev. Lett. 92 (2004) 220601.
[21] B. Jäger, R. Hellmann, E. Bich, E. Vogel, J. Chem. Phys. 135 (2011) 084308.
[22] R. Hellmann, Mol. Phys. 111 (2013) 387–401.
[23] M. P. Vukalovich, Y. F. Masalov, Teploenergetika 13 (1966) 58–62.
[24] J. C. Holste, K. R. Hall, P. T. Eubank, G. Esper, M. Q. Watson, W. Warowny, D. M. Bailey, J. G. Young, M. T. Bellomy, J. Chem. Thermodyn. 19 (1987) 1233–1250.
[25] M. Jaeschke, Int. J. Thermophys. 8 (1987) 81–95.
[26] W. Duschek, R. Kleinrahm, W. Wagner, J. Chem. Thermodyn. 22 (1990) 827–840.
[27] J. H. Dymond, K. N. Marsh, R. C. Wilhoit, K. C. Wong, Landolt-Börnstein: Numerical Data and Functional Relationships in Science and Technology: New Series, volume 21A: Virial Coefficients of Pure Gases of *Group IV: Physical Chemistry*, Springer, Berlin–Heidelberg–New York, 2002, p. 30.
[28] S. Bock, Rechnungen zur Potentialhyperfläche und ausgewählten thermophysikalischen Eigenschaften von Kohlendioxid, Ph.D. thesis, Universität Rostock, Rostock, Germany, 2002.
[29] R. T. Pack, J. Chem. Phys. 78 (1983) 7217–7222.
[30] E. L. Heck, A. S. Dickinson, Physica A 217 (1995) 107–123.
[31] R. Hellmann, E. Bich, E. Vogel, A. S. Dickinson, V. Vesovic, J. Chem. Phys. 129 (2008) 064302.
[32] R. Hellmann, E. Bich, Mol. Phys. (in press, DOI: 10.1080/00268976.2014.951703).
[33] E. Bich, S. Bock, E. Vogel, Physica A 311 (2002) 59–79.
[34] S. Bock, E. Bich, E. Vogel, A. S. Dickinson, V. Vesovic, J. Chem. Phys. 120 (2004) 7987–7997.

[35] R. Span, W. Wagner, J. Phys. Chem. Ref. Data 25 (1996) 1509–1596.
[36] E. L. Heck, A. S. Dickinson, Comput. Phys. Commun. 95 (1996) 190–220.
[37] G. C. Maitland, E. B. Smith, J. Chim. Phys. Phys.-Chim. Biol. 67 (1970) 631–632.
[38] I. N. Hunter, G. Marsh, G. P. Matthews, E. B. Smith, Int. J. Thermophys. 14 (1993) 819–833.
[39] S. Hendl, A.-K. Neumann, E. Vogel, High Temp. - High Press. 25 (1993) 503–511.
[40] S. Bock, E. Bich, E. Vogel, A. S. Dickinson, V. Vesovic, J. Chem. Phys. 117 (2002) 2151–2160.
[41] E. Vogel, private communication, 2014.
[42] E. Bich, R. Hellmann, E. Vogel, Mol. Phys. 105 (2007) 3035–3049.
[43] H. L. Johnston, E. R. Grilly, J. Chem. Phys. 14 (1946) 233–238.
[44] J. W. Haarman, Am. Inst. Phys. Conf. Proc. 11 (1973) 193–198.
[45] A. I. Johns, S. Rashid, J. T. R. Watson, A. A. Clifford, J. Chem. Soc., Faraday Trans. 1 82 (1986) 2235–2246.
[46] J. Millat, M. Mustafa, M. Ross, W. A. Wakeham, M. Zalaf, Physica A 145 (1987) 461–497.
[47] S. F. Y. Li, M. Papadaki, W. A. Wakeham, in: T. W. Tong (Ed.), Proc. 22nd International Thermal Conductivity Conference, (Tempe, Arizona, 1993), Technomic Publishing Company, Lancaster, PA, 1994, pp. 531–543.
[48] V. Vesovic, W. A. Wakeham, G. A. Olchowy, J. V. Sengers, J. T. R. Watson, J. Millat, J. Phys. Chem. Ref. Data 19 (1990) 763–808.
[49] E. Vogel, B. Jäger, R. Hellmann, E. Bich, Mol. Phys. 108 (2010) 3335–3352.
[50] J. O. Hirschfelder, J. Chem. Phys. 26 (1957) 274–281.